Numerical Analysis of Jet-Stirred Reactors with Turbulent Flows and Homogeneous Reactions

A computer program designed to model the turbulent reacting flow in jet-stirred reactors has been developed. In solving the single-phase flow field, a two-equation turbulence closure was used to predict the turbulent eddy viscosity variation in the reactor. The model was used to predict the performance of a real reactor. The predicted results compared favorably with measurements in the field. It was found that the key to the reactor performance is the strength of the recirculating eddy caused by the jet entrainment.

Chih-Hsiung Liu, C. H. Barkelew
Shell Development Company
Houston, TX 77001

Introduction

We have developed a general-purpose computer program to model turbulent, reacting flow systems in two-dimensional (plane, axisymmetric, or polar) geometries. The program is structured in such a way that its main body remains fixed for the class of problems it is designed to solve. For each individual problem we need only to construct an application routine to specify the geometry, boundary conditions, physical properties, and reaction kinetics. This approach is motivated by the need to study a wide variety of process reactors in our plants.

To demonstrate the capability of the program, it was compared to a jet-stirred reactor at one of our refineries. By comparing the calculated results with available observations, we conclude:

1. The model is capable of predicting changes of flow pattern and yield structure in different geometries or operating conditions. The model can be used as an alternative to field trials.
2. The yield structure of the reaction can be slightly changed by making the reactor wider, but not significantly by changing the initial jet conditions, for example by extending the inlet tube or adding swirl.
3. Other jet-stirred reactors for different products can also be simulated and scaled-up with confidence, provided that the reaction kinetics are known.

We are very encouraged by the favorable comparison of predictions with field results. The ability of the program to predict the circulation strength adds a new avenue to the understanding of jet-stirred reactors, to the extent that we can now scale them with confidence.

Correspondence concerning this paper should be addressed to C. H. Liu.

Description of General-Purpose Program

The program is designed to seek numerical solutions for a set of partial differential equations of the following form:

$$\frac{\partial \rho\phi}{\partial t} + \nabla \cdot (\rho V\phi) = \nabla \cdot (\Gamma_\phi \nabla\phi) + S \qquad (1)$$

where $\phi = \phi(x, y, t)$ is any field variable dependent on the time t and the two spatial coordinates x, y. The density is denoted by ρ. The local velocity vector is V and Γ_ϕ is the coefficient of diffusion for ϕ. It will be shown later that the problem under consideration is indeed governed by equations similar to Eq. 1.

The solution method is a control-volume based, finite-difference scheme that follows the Patankar-Spalding (1972) approach. In forming the corresponding difference equations, we weight the contributions from convective and diffusive fluxes across a control volume face, Figure 1, in such a way that the sum of the two is preserved between two adjacent grid points. This scheme (Liu, 1977) is a reasonable compromise between the well-known central difference and upwind difference schemes. The set of difference equations is solved by a conjugate gradient method with incomplete LU (lower/upper) decompositions (LUCG; Meijerink and Vorst, 1977; Kershaw, 1978). To deal with the implicitly coupled pressure and velocity, the SIMPLE (semi-implicit method for pressure-linked equations) method proposed by Caretto et al. (1972) is adopted.

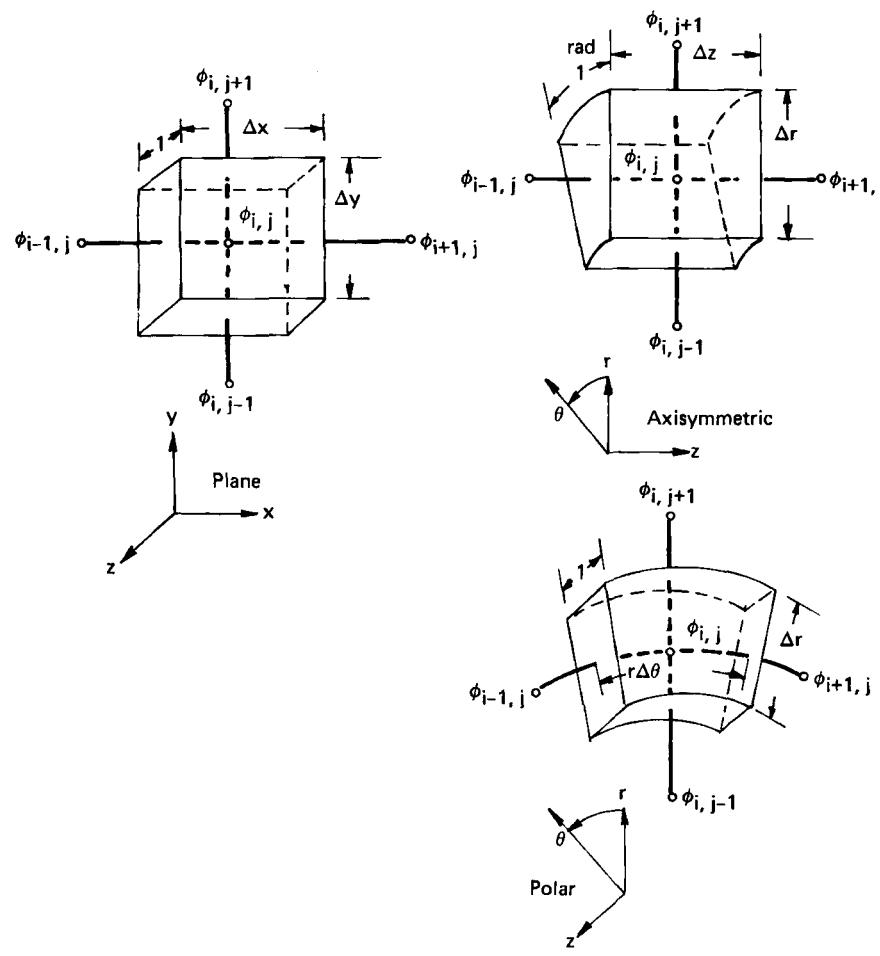

Figure 1. Control volumes in different geometries.

Following the above guidelines, a general-purpose computer program was coded in FORTRAN language. The program consists of two parts: a main body that has a fairly general framework to embody a great variety of problems, and an application-oriented routine to specify the nature of a particular problem we are interested in.

Formulation of the Reactor Problem

For proprietary reasons, we cannot be specific about the details of the process or the reactions that take place. However, we believe that our disguises do not detract from the general utility of the procedure we describe.

The reactor, Figure 2, is a cylindrical vessel whose length and diameter are L and D, respectively. The reactants, A and B, are premixed and fed at near sonic velocity through an inlet pipe of diameter d. The product leaves the vessel through a pipe of diameter d_e. In our simulation, we have represented the real ellipsoidal heads at the ends of the vessel as planar. Heat losses through the wall have been neglected.

By affixing a coordinate system (x, r) at the inlet of the reactor, the governing equations for the momentum, heat, and mass transfers can be cast into a general form similar to Eq. 1. Table 1 lists the respective terms in the general equations for each of the variables to be solved; u, v, and w are the axial, radial, and swirling velocity components, respectively. The equivalent pressure $\tilde{P}$ is equal to $P + [2\mu(\nabla \cdot V)/3] + (2\rho k/3)$. The two variables k and ϵ represent the so-called two-equation model for turbulence (Launder and Spalding, 1972, 1974) from which the equivalent turbulent viscosity μ_{eff} can be derived:

$$\mu_{\text{eff}} = C_D \cdot \rho \cdot k^2/\epsilon \tag{2}$$

C_D is an empirical constant whose value is given in Table 2. The total viscosity μ_t is the sum of laminar viscosity μ and μ_{eff}. The adoption of the two-equation turbulence model is recommended by Harsha (1971), who has compared extensive experimental data with predictions based on several turbulence models for jet mixing problems. In the two equations for k and ϵ, there is a turbulence generation term:

$$G = \mu_t \left\{ 2\left[\left(\frac{\partial u}{\partial x}\right)^2 + \left(\frac{\partial v}{\partial r}\right)^2 \right] + \left(\frac{\partial w}{\partial x}\right)^2 + \left[r\frac{\partial}{\partial r}\left(\frac{w}{r}\right) \right]^2 + \left(\frac{\partial u}{\partial r} + \frac{\partial v}{\partial x}\right)^2 + \frac{2v^2}{r^2} \right\} \tag{3}$$

Two more constants, C_1 and C_2, are introduced; their values are listed in Table 2. For swirling flows, the constant C_2 should be multiplied by a factor $(1 - 0.20\ Rn)$, where the Richardson

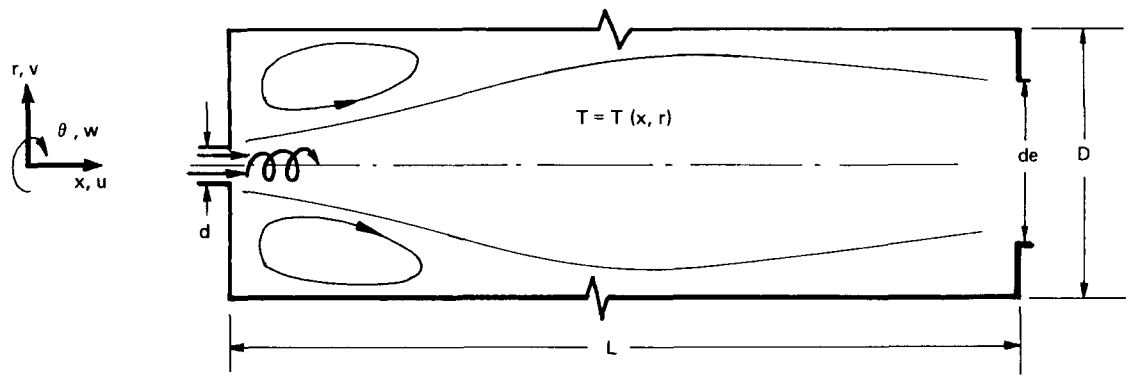

Figure 2. Reactor model.

number Rn is given by

$$Rn = \frac{k^2}{\epsilon^2}\frac{w}{r^2}\frac{\partial(rw)}{\partial r} \tag{4}$$

The above modification is based on the work of Priddin (1985), Bradshaw (1973), and Koosinlin et al. (1974). The source term ΔH in the equation for the stagnation enthalpy, h, represents the total heat of reaction. We have neglected the contributions to the energy flux from the interdiffusion of different species and the diffusion-thermo effect. In the actual program implementation, we choose to use the local temperature T as the active variable. The arrays that store ρ and Γ_ϕ are both temporarily multiplied by the specific heat, C_p, when this equation is solved. The last equation in Table 1 is a general form for the mass transfer equation governing each chemical species being considered. The actual reaction chains are rather involved and would require too much computer time for a complete analysis. Therefore, only the following three major reactions are considered here.

$$A + B \rightarrow C + D \tag{5a}$$

$$D + B \rightarrow E + C \tag{5b}$$

$$A + B \rightarrow F \tag{5c}$$

Species D is the desired product. Species C is a by-product of no value, one that is easily separated and disposed of. Species E and F are by-products of significant but different values.

Since C_i in Table 1 represents any of the above six species, there are six component equations to be solved. Although the convection and turbulent diffusion for these six species are similar, the source terms are quite different due to the fact that the three reactions, Eqs. 5a–5c, have different rate expressions. Table 3 summarizes the $\dot{C}_i$ used in the calculation.

In the formulation, all of the species concentrations are in mole fractions, and the temperature is in Kelvins. The rate constants α_i are measured values. Their orders of magnitudes are: $\alpha_1 = 0(1)$, $\alpha_2 = 0(-2)$, $\alpha_3 = 0(4)$, α_4 to $\alpha_6 = 0(-6)$. The Arrhenius temperature coefficients, E_i, range from 10^3 to 10^4. The boundary conditions pertaining to the aforementioned problem are: The inlet conditions are known; the normal gradients are assumed vanishing along the axis and the exit. The wall is impermeable and thermally insulated. To simulate the laminar sublayer for the flow fields without excessive use of grid points near the wall, the wall function deduced by Spalding (1961) and Kleinstein (1967) is adopted for the control volumes adjacent to the wall.

The set of equations in Table 1 and the aforementioned boundary conditions form a complete mathematical description of the reactor problem being considered. Since the entire system is

Table 1. General Equation Terms for Dependent Field Variables

Variable ϕ	Coeff. of Turbulent Diffusion Γ_ϕ	Generalized Source Term S
1	0	0
u	μ_t	$-\frac{\partial \tilde{P}}{\partial x} + \frac{\partial}{\partial x}\left(\mu_t \frac{\partial u}{\partial x}\right) + \frac{1}{r}\frac{\partial}{\partial r}\left(r\,\mu_t \frac{\partial v}{\partial x}\right)$
v	μ_t	$-\frac{\partial \tilde{P}}{\partial r} + \frac{\partial}{\partial x}\left(\mu_t \frac{\partial u}{\partial r}\right) + \frac{1}{r}\frac{\partial}{\partial r}\left(r\,\mu_t \frac{\partial v}{\partial r}\right) - \frac{2\,\mu_t v}{r^2} + \frac{\rho w^2}{r}$
rw	μ_t	$-\frac{2}{r}\frac{\partial}{\partial r}(\mu_t rw)$
k	μ_t/σ_k	$G - \rho\epsilon$
ϵ	μ_t/σ_ϵ	$(C_1 G - C_2\,\rho\epsilon)\frac{\epsilon}{k}$
h	μ_t/σ_h	ΔH
C_i	μ_t/σ_i	$\rho\dot{C}_i$

Table 2. Numerical Values of Constants

C_D	0.09
C_1	1.44
C_2	1.92
σ_k	1.0
σ_ϵ	1.3
σ_h	0.9
σ_i	0.9

very complex, it is not desirable to tackle the entire problem altogether because of excessive computing costs. In the process reactor, since both the temperature and compressibility effects are small except near the inlet, the density does not vary appreciably in the major portion of the reactor. Hence, the constant-density simplification was adopted and the momentum transfer is completely decoupled. The solutions obtained do indicate that the approximation is reasonable. It should be noted that the program retains the ability to treat variable density flows.

Results and Discussion

The formulation outlined in the preceding section has been coded into two separate user programs, one for momentum transfer, the other for heat and mass transfer. During the execution stage, the former is first linked to the main body, which is common to all of the user-prepared routines. The resulting flow field and turbulence properties are then used as part of the input needed to execute the latter subroutine by linking to the same main program again.

Table 3. $\dot{C}_i$ Used in Reaction Calculations

$$(\dot{A}) = -R_1 - R_3(1 - A)$$
$$(\dot{B}) = -R_1 - R_2 - R_3(1 - B)$$
$$(\dot{C}) = R_1 + R_2 + R_3(C)$$
$$(\dot{D}) = R_1 - R_2 + R_3(D)$$
$$(\dot{E}) = R_2 + R_3(E)$$
$$(\dot{F}) = R_3(1 + F)$$

Where

$$R_1 = (X_7) \cdot (A)$$
$$R_2 = \alpha_1 \cdot (X_7) \cdot (D)$$
$$R_3 = \alpha_2 \cdot (X_6)(X_8)(B)$$

$$X_1 = \alpha_3 \cdot \exp\left(-\frac{E_1}{T}\right)$$

$$X_2 = \alpha_4 \cdot \exp\left(\frac{E_2}{T}\right)$$

$$X_3 = \alpha_5 \cdot \exp\left(\frac{E_3}{T}\right)$$

$$X_6 = \exp\left(\frac{E_4}{T}\right)$$

$$X_7 = X_1 \cdot S_1$$
$$X_8 = S_1 \cdot (A)/(1 + X_3 \cdot B)$$

$$S_1 = 1.0E3 \times (B)^{1.5}/[(1 + X_2 \cdot A) \cdot (A)^{0.5}] \cdot \sqrt{1 + \alpha_6 \exp\left(\frac{E_5}{T}\right)}$$

$$C_p = \partial h/\partial T = C_p(T, C_i)$$

$$\Delta H = \sum_{j=1}^{3} Q_j R_j$$

The solution is based on a 20 × 20 grid system. The nonuniformly distributed grids cluster around the inlet nozzle and the walls, where steep gradients are expected. On our UNIVAC 1184 computer, a typical solution requires about 10 CPU min for the flow calculation and 25 min for the remaining task. The longer execution time for the heat and mass transfer calculations stems from the fact that in order to make a valid comparison among various cases, the inlet temperature has to be varied to yield a fixed outlet temperature. This necessitates repeated applications of the solution procedure through trial and error.

Six different cases have been studied, of which four involve changes in inlet conditions; the remaining two cases are for different reactor sizes. The base case, designated case A, is the existing reactor. Uniform axial sonic velocity is assumed at the inlet. Case B is similar to case A, except that the inlet velocity has a radial component that varies linearly from zero at the axis to half-sonic near the nozzle wall. The additional radial velocity is included to simulate possible formation of an oblique shock at the inlet. Case C is also similar to case A, except that the inlet pipe in the former case is extended into the reactor. Case D is essentially case A with additional swirl introduced in the jet. A constant angular velocity is assumed such that the swirling velocity at the edge of inlet nozzle is half-sonic.

Cases E and F retain the same inlet condition as that of the base case. The dimensions of the reactor, however, have been changed. In case E, the diameter has been increased by 37%. In case F, the length has been decreased by 24% and the diameter increased to preserve the volume. In the following discussion, the resulting flow patterns for these cases will be presented first, followed by temperature distributions and yield profiles.

A useful parameter, known as the Craya-Curtet number, should also be introduced here. This number uniquely describes the similarity principle developed by Craya and Curtet (1955) and Curtet (1958) for an incompressible round jet discharging into a duct fed by a uniform stream. Our jet-stirred reactor is just the limiting case where the feeding stream surrounding the jet nozzle is blocked completely, and consequently

$$C_t = \frac{r_o}{\sqrt{r_w^2 - \frac{1}{2}r_o^2}} \tag{6}$$

where r_o and r_w are the radii of the nozzle and vessel wall, respectively.

The calculated flow pattern for case A is plotted in Figure 3A. Only half of the vessel is shown because of symmetry. The stream function ψ is normalized by ψ_o, which is related to the reactor throughput $\dot{M}$ by:

$$\dot{M} = 2\pi\psi_o \tag{7}$$

The main jet expands once it leaves the nozzle. The expanding action causes an adverse pressure gradient that induces a recirculation eddy along the side wall. The expansion of the jet can be characterized by how rapidly the axial velocity decays, as shown in Figure 4. The measurements made by Becker et al. (1963) for three different C_t = 0.0325, 0.18, 0.345 are also cited in the same figure. The Craya-Curtet number for case A is 0.11. It

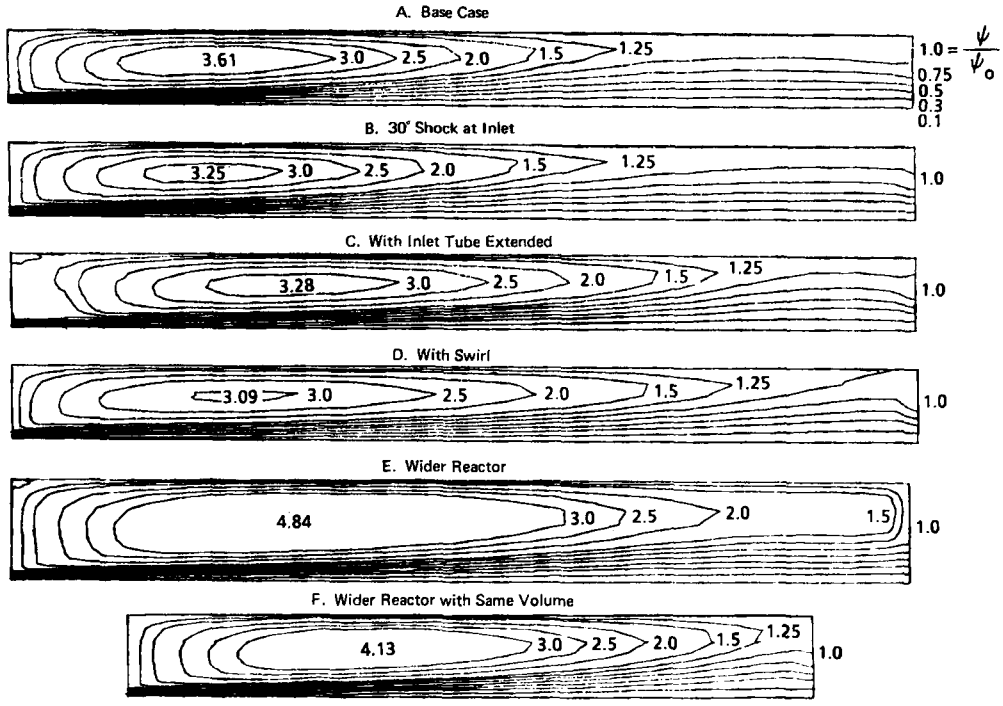

Figure 3. Flow patterns for various cases.

should be pointed out that the axial velocity has been normalized by the same characteristic velocity u_o^* given by Becker et al. The u_o^* is related to the mean jet velocity at the nozzle, u_o, by

$$u_o^* = \frac{1}{C_t}\frac{r_o^2}{r_w^2}u_o \tag{8}$$

The axial velocity decay rate predicted by the model is generally slower than the observed rate for corresponding C_t. The model, however, does predict the change in the decaying slope near $u_o/u_c^* = 2.4$. Such a change in slope has been specially noted by Becker and is attributed to the presence of the recirculation eddy. Indeed, the decaying curves for free jets do not have such a marked changing point.

Properties of the recirculation eddy are also of special interest since they have long been perceived as the key to variations in the yield structure of jet-stirred reactors. The recirculation strength, which is characterized by the total mass flow rate in the recirculation eddy, can be obtained by subtracting ψ_o from the maximum of ψ, i.e.,

$$\psi_{\text{eddy}} = \psi_{\max} - \psi_o \tag{9}$$

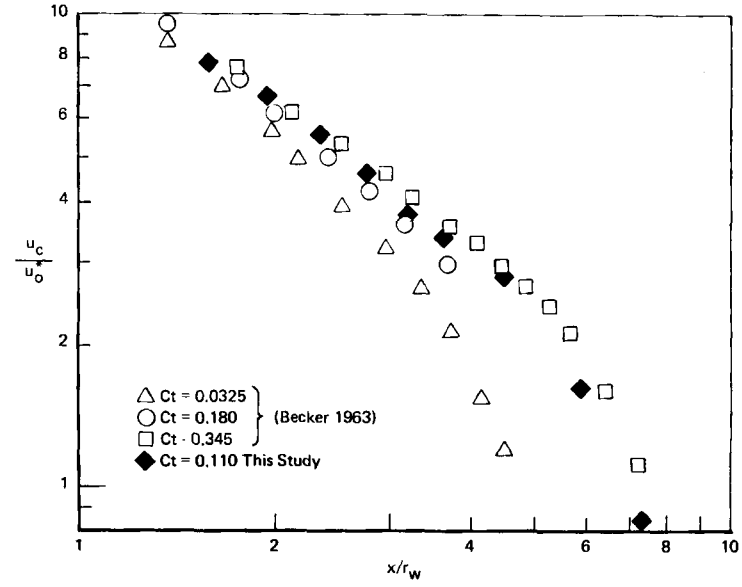

Figure 4. Comparison of center-line velocity decay in confined jets.

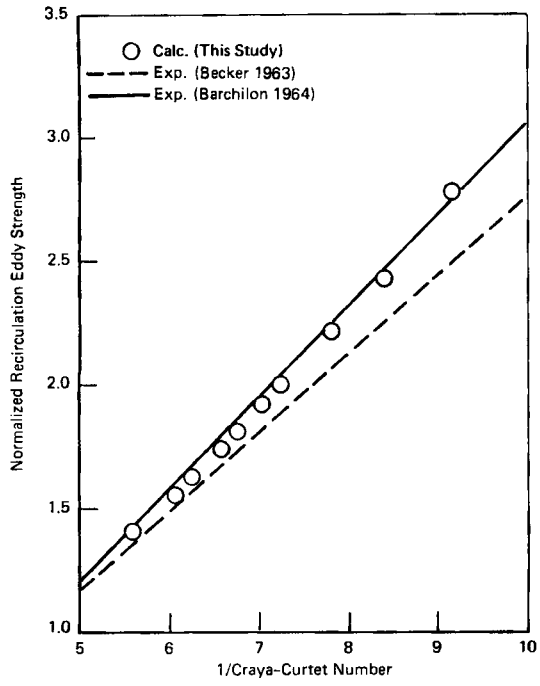

Figure 5. Comparison between predicted recirculation strength and experimental data.

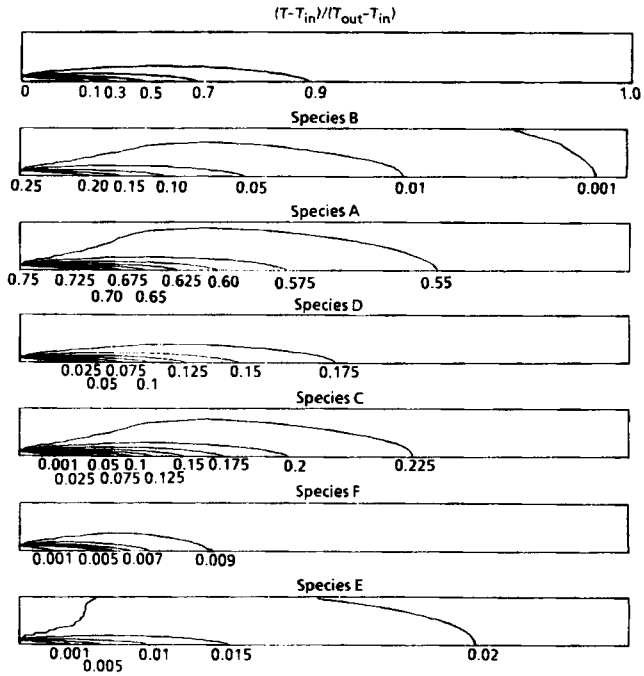

Figure 6. Temperature and species concentrations.

Becker et al. establish a correlation between ψ_{eddy} and C_t from his experiments.

$$\frac{\psi_{eddy}}{\psi_o} = \frac{0.32}{C_t} - 0.43 \tag{10}$$

A similar experiment has also been conducted by Barchilon and Curtet (1964). They did not report the recirculation strength in full detail. In fact, only three data points were shown in Figure 4 of their report. The three data points, however, lie on a straight line and can be approximated by:

$$\frac{\psi_{eddy}}{\psi_o} = \frac{0.37}{C_t} - 0.64 \tag{11}$$

A comparison among the ψ_{eddy} values predicted by the program and those based on Eqs. 10 and 11 is made in Figure 5. It is seen that the predicted recirculation strength comes very close to the observation. Furthermore, the predicted values fall between the two sets of measurements. Since the two experiments show about 10% difference in results, which could be due to subtle

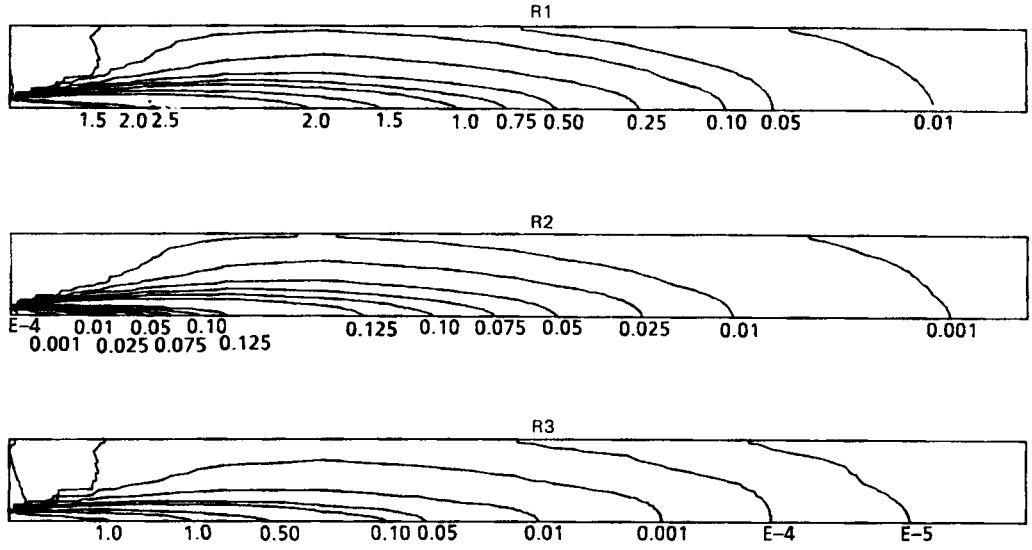

Figure 7. Distributions of the rates of three major reactions.

Table 4. Concentrations in Product

Species	Measured Field Data	Calculated					
		Case A	Case B	Case C	Case D	Case E	Case F
		$T_{out} - T_{in}$					
	280	271	271	276	270	270	267
B	4.35E-4	8.31E-4	8.91E-4	1.53E-3	2.07E-3	1.43E-3	3.66E-3
A	5.42E-1	5.45E-1	5.49E-1	5.29E-1	5.50E-1	5.45E-1	5.48E-1
D	1.86E-1	1.92E-1	1.91E-1	1.96E-1	1.89E-1	1.91E-1	1.89E-1
C	2.34E-1	2.33E-1	2.30E-1	2.40E-1	2.28E-1	2.32E-1	2.29E-1
F	9.5E-1	9.35E-3	1.09E-2	1.22E-2	1.09E-2	8.97E-3	9.13E-3
E	1.55E-2	2.03E-2	1.95E-2	2.16E-2	1.94E-2	2.05E-2	2.00E-2
		ψ_{eddy}/ψ_o					
		2.61	2.25	2.28	2.09	3.84	3.13

variations in the experimental setup, it is felt that the prediction is adequate and no further refinement in the model is required.

Other information of secondary importance, such as the axial location of the center of the recirculation eddy (χ_{eddy}), has also been reported by Becker et al. and by Barchilon and Curtet. For $C_t = 0.08$ to 0.11, χ_{eddy}/r_w is about 3.2 to 3.3 from observation. The present calculation is in agreement with this value. The reattachment point of the recirculation eddy on the wall, according to Barchilon and Curtet, is about 6.25 r_w regardless of C_t. The present calculations do not show the same effect. This discrepancy could be due to the fact that the experiment is based on a very long pipe while the reactor currently considered is of finite length and has a neck-down at the exit. Recirculation patterns similar to our predictions have also been observed in model furnaces with exit neck-down built by SOGREAH Laboratories in Grenoble, France, for the International Flame Research Foundation (Curtet, 1958).

To complete the report on flow patterns, Figures 3B to 3F show the streamlines for cases B through F, respectively. Their overall patterns are quite similar, but the rates of the recirculation eddies differ substantially.

The calculated temperature and mole fractions for case A are shown in Figure 6. It is seen that the temperature rises rapidly near the jet inlet and that for most of the reactor it is close to that of the exit. This supports the earlier assumption that density variations can be neglected. The three reaction rates R_1, R_2, R_3 are shown in Figure 7.

The calculated model concentrations in the product are summarized in Table 4, along with a set of measured values. The agreement is entirely satisfactory, considering the simplified model of the reaction kinetics that was used.

It is reasonable to conclude that insofar as this process is concerned, the results of these calculations are in good agreement with observations. What the procedure provides that we did not have before is the ability to predict the strength of the recirculation for a variety of reactor configurations. Thus, divergence of the jet, swirl in the jet, or a reentrant feed port all decrease the circulation strength, and would be expected to have a corresponding effect on the composition of the product. Increasing the reactor diameter increases the circulation.

Encouraged by the favorable results, we are currently extending the computer model to two-phase flow systems (Liu and Tulig, 1985). This modeling effort is further supplemented by experimental work in our laboratory (Berker et al., 1985).

Notation

C_i = species concentration in mole fraction, mol/mol
$\dot{C}_i$ = rate of change of species concentration, 1/s
C_p = specific heat, J/kg · K
C_t = Craya-Curtet number
E_i = Arrhenius temperature coefficient, Table 3, 1/K
G = turbulence generation term, N/m^2 · s
h = stagnation enthalpy, J/kg
k = turbulent kinetic energy, m^2/s^2
P = pressure, N/m^2
$\tilde{P}$ = equivalent pressure, N/m^2
Q_j = heat formation of jth reaction, J/mol
R_j = rate of jth reaction, mol/s
R_n = Richardson number
r = radial coordinate, m
r_o = radius of inlet nozzle, m
r_w = radius of cylindrical vessel, m
S = generalized source term
T = temperature, K
t = time, s
u = axial velocity, m/s
u_o = inlet velocity, m/s
u_o^* = characteristic velocity, m/s
$\vec{V}$ = velocity vector, m/s
v = radial velocity, m/s
w = swirling velocity, m/s
x = axial coordinate, m
y = coordinate perpendicular to x, m

Greek letters

α_i = rate constant, mol/s
ϵ = eddy dissipation rate, m^2/s^3
μ = laminar viscosity, N · s/m^2
μ_{eff} = effective turbulent viscosity, N · s/m^2
$\mu_t = \mu + \mu_{eff}$, N · s/m^2
ρ = density, kg/m^3
σ_ϕ = turbulent Prandtl or Schmidt number for ϕ
ϕ = dependent field variable
χ_{eddy} = axial location of center of recirculation eddy, m
ψ = stream function, kg/s
ψ_o = inlet stream function, kg/s
ψ_{eddy} = mass flow rate of recirculation eddy, kg/s
Γ_ϕ = coefficient of turbulent diffusion for ϕ
ΔH = net heat formation of reactions, J/s

Literature cited

Barchilon, M., and R. Curtet, "Some Details of the Structure of an Axisymmetric Confined Jet with Backflow," *J. Basic Eng.*, **86**, 777 (1964).

Becker, H. A., H. C. Hottel, and G. C. Williams, "Mixing and Flow in Ducted Turbulent Jets," *9th Symp. Combustion*, Academic Press, London, 7 (1963).

Berker, A., C. H. Barkelew, and C. H. Liu, "Two-phase Flow Measurements Using a Gamma Camera—Density and Velocity Distributions in Gas-Solid Systems," *AIChE Ann. Meet.*, Chicago (Nov., 1985).

Bradshaw, P., "The Effects of Streamline Curvature on Turbulent Flow," AGARDO Graph No. 169 (1973).

Caretto, L. S., A. D. Gosman, S. V. Patankar, and D. B. Spalding, "Two Calculation Procedures for Steady, Three-Dimensional Flows with Recirculation," *Proc. 3rd Int. Conf. Num. Methods in Fluid Dynamics*, Paris (July, 1972).

Craya, A., and R. Curtet, "On the Spreading of a Confined Jet," *Comptes Rendus Acad. des Sciences*, Paris, **241**, 621 (1955).

Curtet, R., "Confined Jets and Recirculation Phenomena with Cold Air," *Combustion and Flame*, **2**(4), 383 (1958).

Harsha, P. T., "Free Turbulent Mixing: A Critical Evaluation of Theory

and Experiment," Arnold Eng. Dev. Center AEDC-TR-71-36 (1971).

Kershaw, D. S., "The Incomplete Cholesky-Conjugate Gradient Method for the Iterative Solution of Systems of Linear Equations," *J. Comp. Phy.*, **26**, 43 (1978).

Kleinstein, G., "Generalized Law of the Wall and Eddy—Viscosity Model for Wall Boundary Layers," *AIAA J.*, **5**(8), 1402 (1967).

Koosinlin, M. L., B. E. Launder, and B. I. Sharma, "Prediction of Momentum, Heat and Mass Transfer in Swirling Turbulent Boundary Layers," *J. Heat Transfer*, **96**, 204 (1974).

Launder, B. E., and D. B. Spalding, *Mathematical Models of Turbulence*, Academic Press (1972).

———, "The Numerical Computation of Turbulent Flows," *Comp. Meth. Appl. Mech. Eng.* **3**, 269 (1974).

Liu, C. H., "Numerical Analysis of the Anode Region of High-Intensity Arcs," Heat Transfer Div., Univ. Minnesota (1977).

Liu, C. H., and T. J. Tulig, "A Computer Model for Dispersed Fluid-Solid Turbulent Flows," *AIChE Ann. Meet.*, Chicago, (Nov., 1985).

Meijernik, J. A., and H. A. van der Vorst, "An Interactive Solution Method for Linear Systems of which the Coefficient Matrix is a Symmetric *M* Matrix," *Math. of Comp.*, **31**(137), 148 (1977).

Patankar, S. V., and D. B. Spalding, "A Calculation Procedure for Heat, Mass and Momentum Transfer in Three-Dimensional Parabolic Flows," *Int. J. Heat Mass Transfer*, **15**, 1787 (1972).

Priddin, C. H., "The Behaviour of the Turbulent Boundary Layer on Curved Porous Walls," Ph.D. Diss., Univ. London (1985).

Spalding, D. B., "A Single Formula for the Law of the Wall," *J. Appl. Mech.*, **28**, 455 (1961).

Manuscript received May 6, 1985, and revision received Jan. 13, 1986.